Elastic and anelastic anomalies in (Ca,Sr)TiO perovskites: Analogue behaviour for silicate perovskites

J.W. Walsh, P.A. Taylor, A. Buckley, T.W. Darling, J. Schreuer, M.A. Carpenter

▶ **To cite this version:**

J.W. Walsh, P.A. Taylor, A. Buckley, T.W. Darling, J. Schreuer, et al.. Elastic and anelastic anomalies in (Ca,Sr)TiO perovskites: Analogue behaviour for silicate perovskites. Physics of the Earth and Planetary Interiors, 2008, 167 (1-2), pp.110. ⟨10.1016/j.pepi.2008.02.009⟩. ⟨hal-00532139⟩

HAL Id: hal-00532139

https://hal.science/hal-00532139v1

Submitted on 4 Nov 2010

HAL is a multi-disciplinary open access archive for the deposit and dissemination of scientific research documents, whether they are published or not. The documents may come from teaching and research institutions in France or abroad, or from public or private research centers.

L'archive ouverte pluridisciplinaire **HAL**, est destinée au dépôt et à la diffusion de documents scientifiques de niveau recherche, publiés ou non, émanant des établissements d'enseignement et de recherche français ou étrangers, des laboratoires publics ou privés.

HAL Authorization

Accepted Manuscript

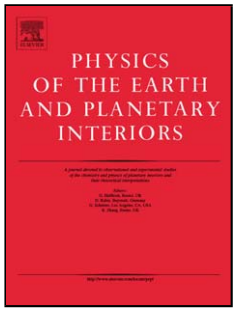

Title: Elastic and anelastic anomalies in $(Ca,Sr)TiO_3$ perovskites: Analogue behaviour for silicate perovskites

Authors: J.W. Walsh, P.A. Taylor, A. Buckley, T.W. Darling, J. Schreuer, M.A. Carpenter

PII: S0031-9201(08)00038-1
DOI: doi:10.1016/j.pepi.2008.02.009
Reference: PEPI 4906

To appear in: *Physics of the Earth and Planetary Interiors*

Received date: 30-10-2007
Revised date: 18-2-2008
Accepted date: 27-2-2008

Please cite this article as: Walsh, J.W., Taylor, P.A., Buckley, A., Darling, T.W., Schreuer, J., Carpenter, M.A., Elastic and anelastic anomalies in $(Ca,Sr)TiO_3$ perovskites: Analogue behaviour for silicate perovskites, *Physics of the Earth and Planetary Interiors* (2007), doi:10.1016/j.pepi.2008.02.009

This is a PDF file of an unedited manuscript that has been accepted for publication. As a service to our customers we are providing this early version of the manuscript. The manuscript will undergo copyediting, typesetting, and review of the resulting proof before it is published in its final form. Please note that during the production process errors may be discovered which could affect the content, and all legal disclaimers that apply to the journal pertain.

ACCEPTED MANUSCRIPT

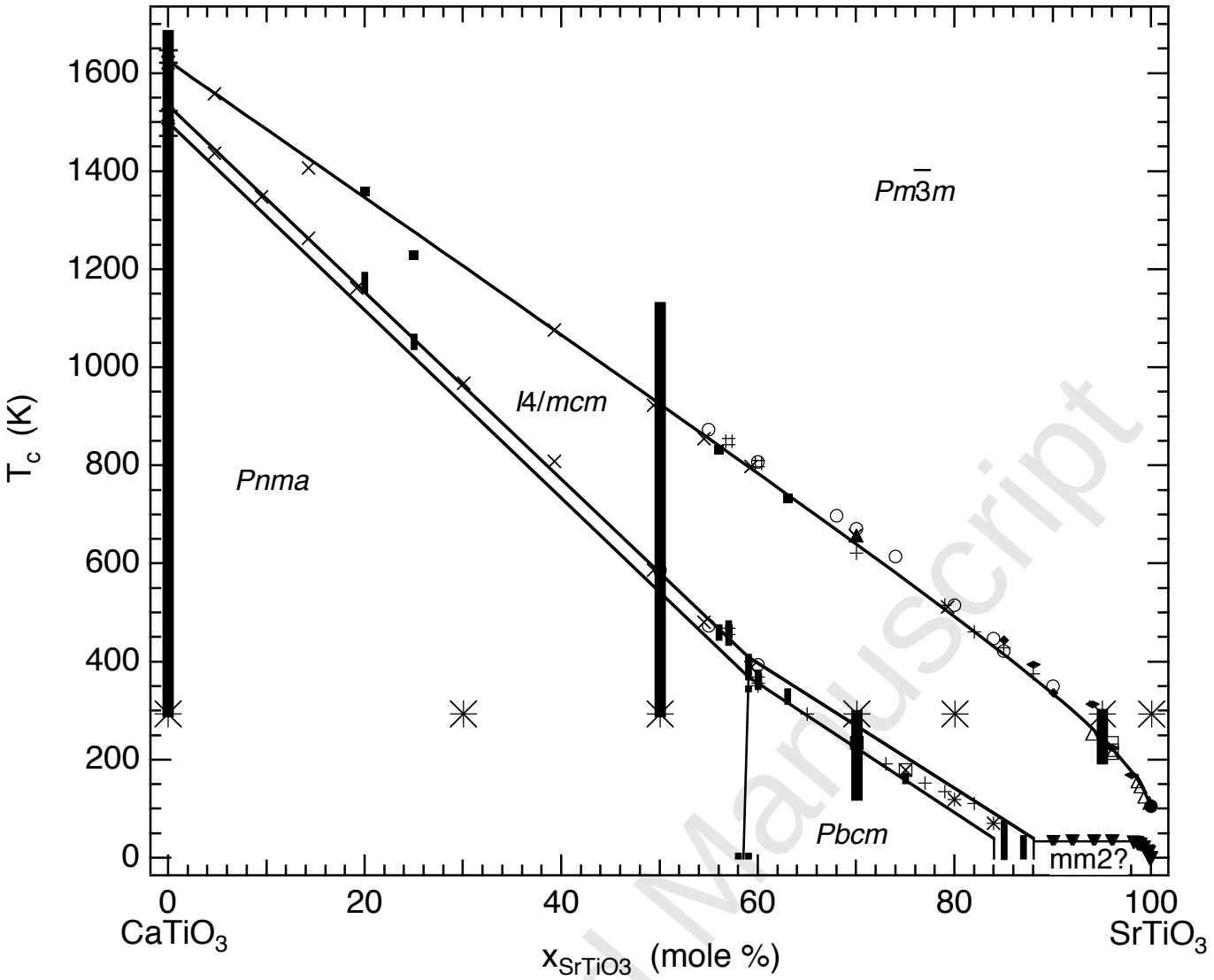

Accepted Manuscript

ACCEPTED MANUSCRIPT

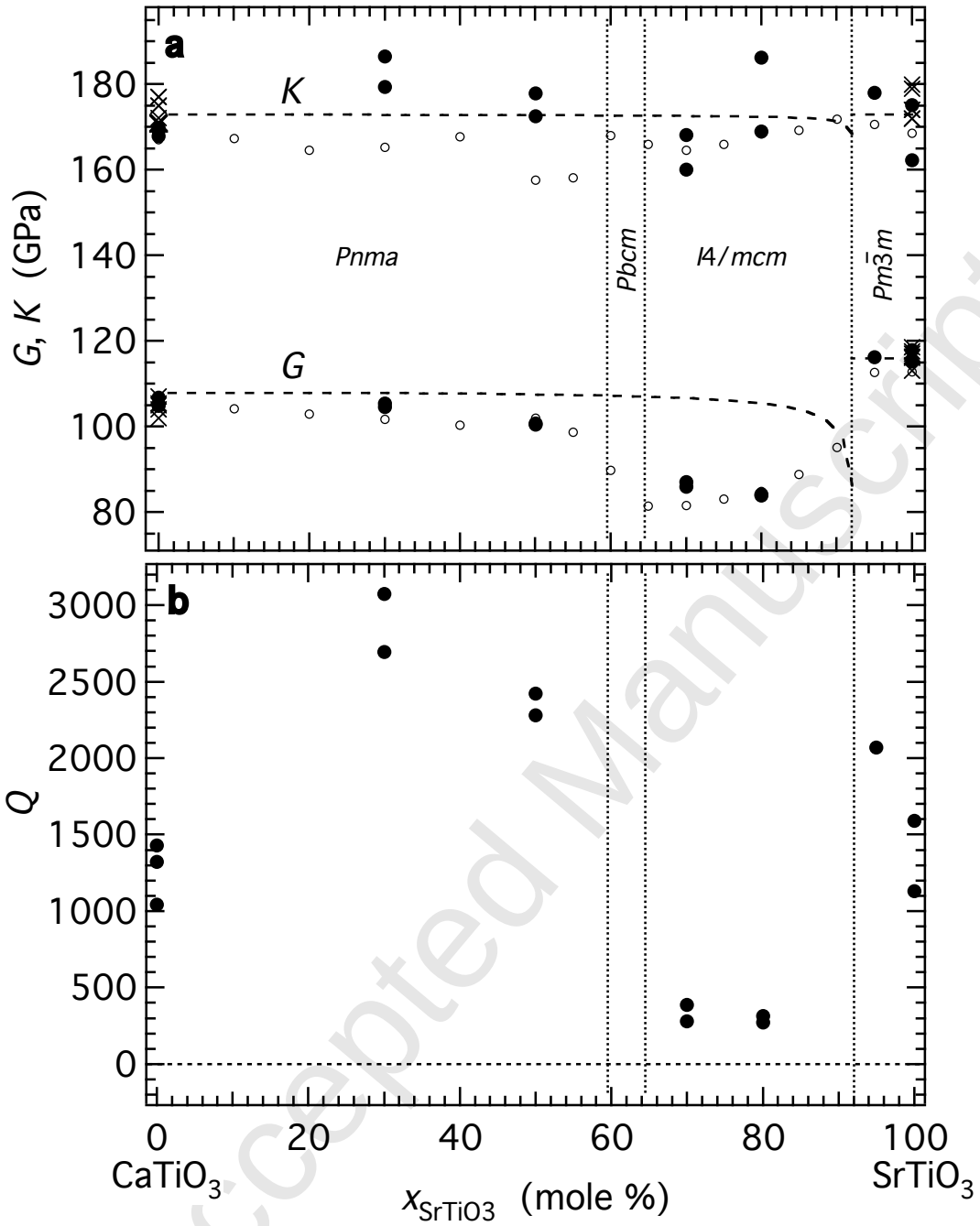

Accepted Manuscript

ACCEPTED MANUSCRIPT

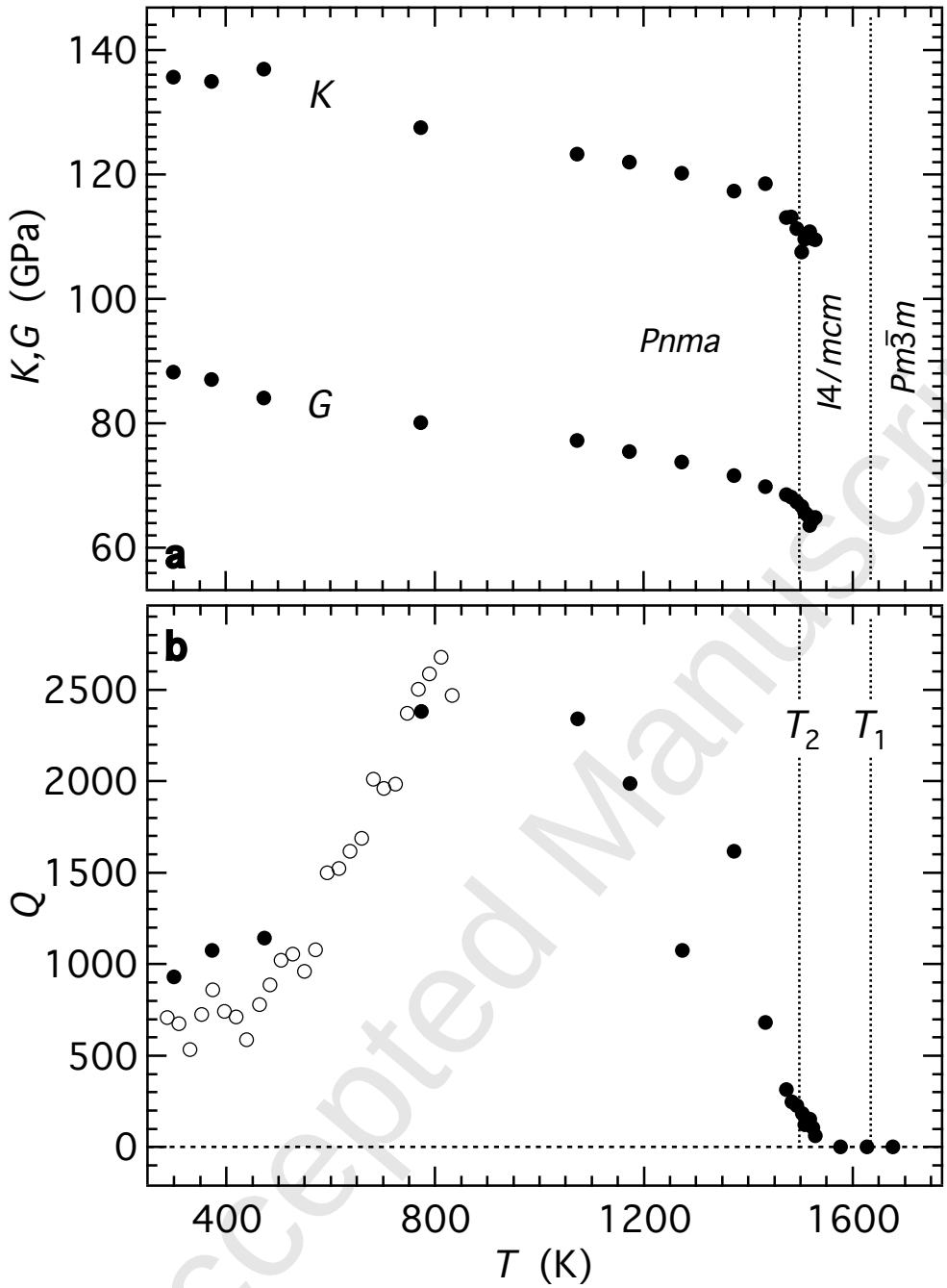

Accepted Manuscript

ACCEPTED MANUSCRIPT

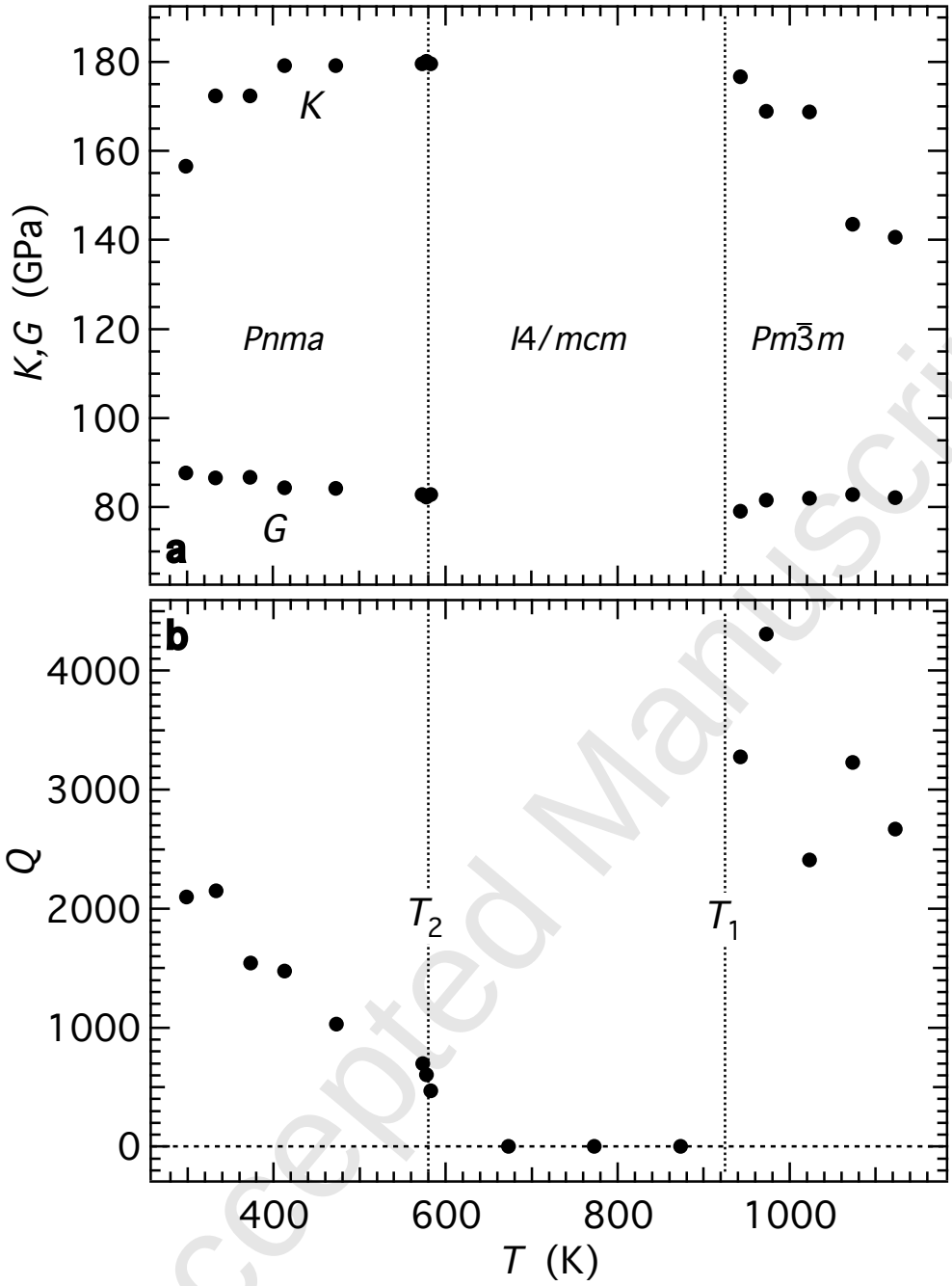

Accepted Manuscript

ACCEPTED MANUSCRIPT

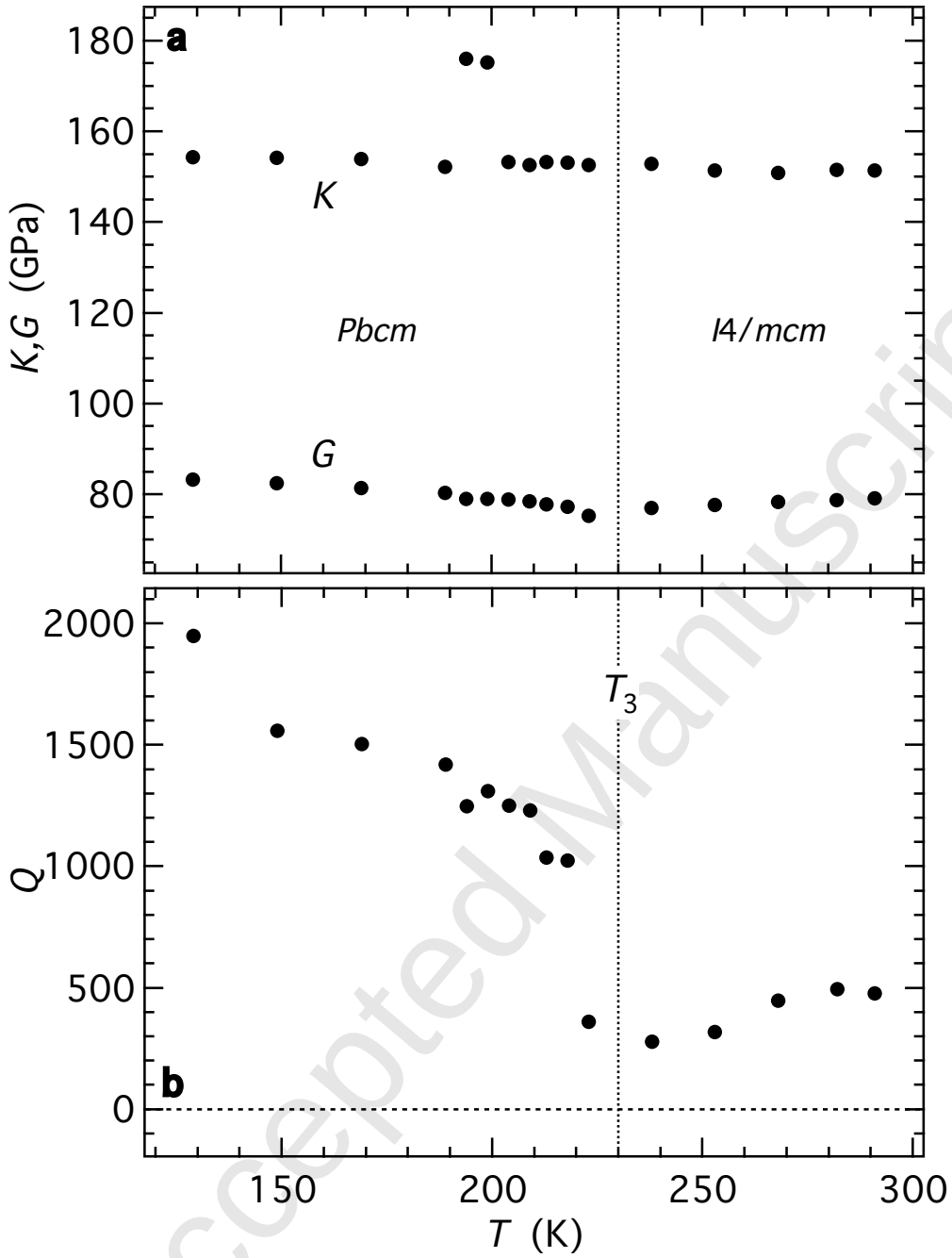

Accepted Manuscript

ACCEPTED MANUSCRIPT

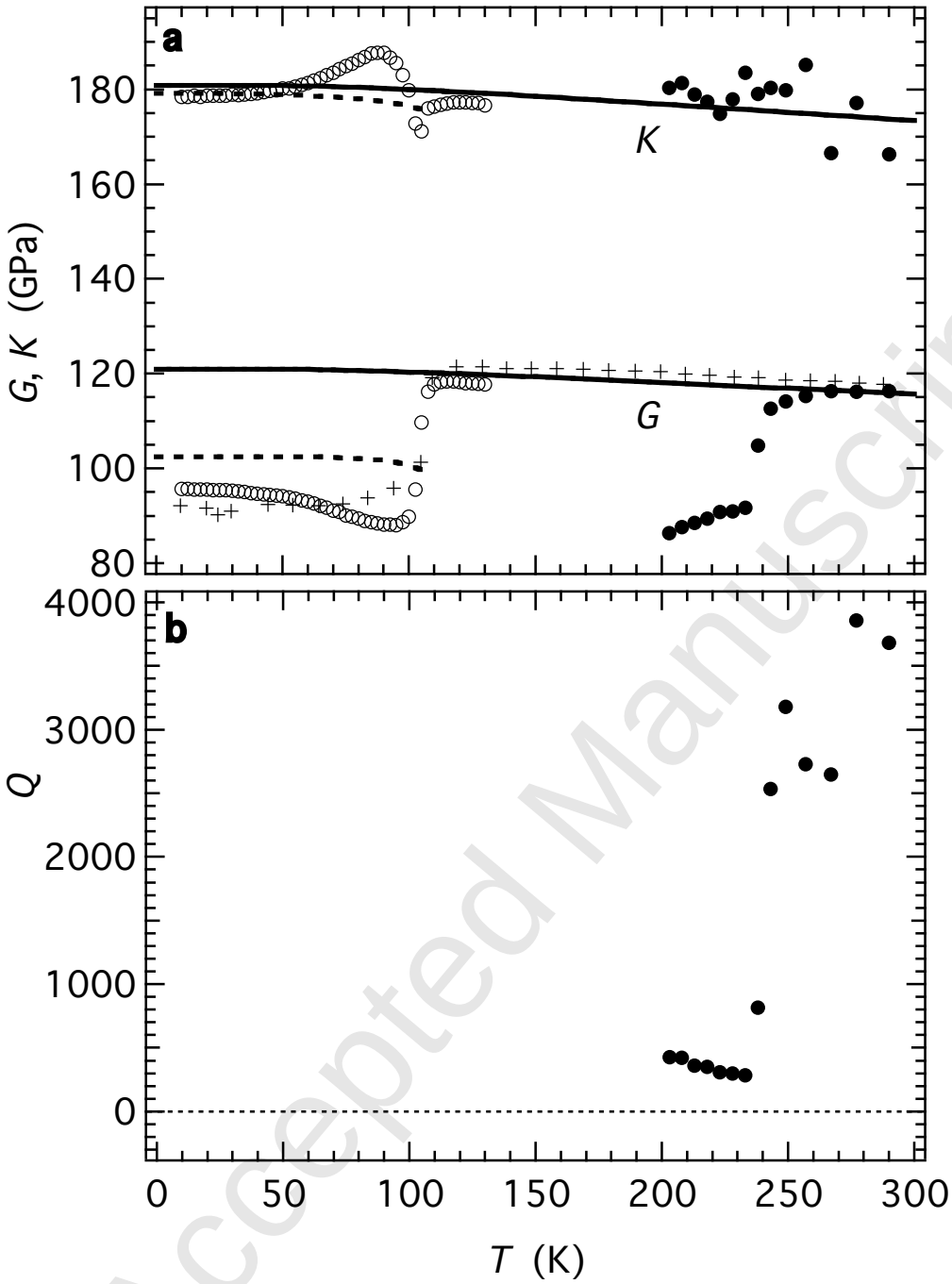

Accepted Manuscript

* Manuscript
ACCEPTED MANUSCRIPT

Elastic and anelastic anomalies in (Ca,Sr)TiO_3 perovskites: analogue behaviour for silicate perovskites

J.W.Walsh[a], P.A.Taylor[a], A.Buckley[a], T.W.Darling[b], J.Schreuer[c], M.A.Carpenter[a]

[a]Dept. of Earth Sciences, University of Cambridge, Downing Street, Cambridge CB2 3EQ, UK

[b]Dept. of Physics, University of Nevada, Reno, NV89577, U.S.A.

[c]Ruhr-Universität Bochum, Institute of Geology, Mineralogy and Geophysics, D-44780, Bochum, Germany

Abstract

Values of bulk modulus (K), shear modulus (G) and mechanical quality factor (Q) have been determined for polycrystalline samples across the $CaTiO_3$ (CST0) – $SrTiO_3$ (CST100) solid solution by Resonant Ultrasound Spectroscopy. Because of similarities with low frequency elastic and anelastic anomalies due to twin wall motion reported in previous studies, a working hypothesis is developed in which dissipation processes are interpreted in terms of twin wall displacements. At high temperatures in CST50 the stability field of the $I4/mcm$ structure is marked by the disappearance of all resonance peaks (superattenuation). This is attributed to anelastic domain wall sliding. At room temperature the $I4/mcm$ phase of CST70 and CST80 has values of G which are lower than those of cubic or orthorhombic phases, and a concomitant drop in Q is interpreted as implying that the domain wall pinning process reported elsewhere to occur below ~400-450 K is only partial. A similar drop in G and Q was found in CST95 below the $Pm\bar{3}m \leftrightarrow I4/mcm$ transition at ~238 K. The $I4/mcm \leftrightarrow Pbcm$ transition in CST70 at ~230 K is marked by an abrupt increase in Q, suggesting that

Accepted Manuscript

ACCEPTED MANUSCRIPT

mobile twins in crystals with the *I*4/*mcm* structure become effectively immobile in antiferroelectric crystals with the *Pbcm* structure. The *I*4/*mcm* ↔ *Pnma* transition in CST50 is marked by a similarly abrupt increase in *Q*, consistent with twin walls becoming effectively immobile also in crystals with the *Pnma* structure. A fall in *Q* below ~800 K in CST0, however, could imply that a degree of twin wall mobility might develop in *Pnma* crystals if the tetragonal spontaneous strain departs significantly from zero. The remarkable attenuation behaviour of crystals with the *I*4/*mcm* structure at the relatively low stress conditions which apply during resonances of a parallelepiped with edge dimensions of ~2-4 mm, is consistent with the view that a characteristic signature for tetragonal $CaSiO_3$ in the earth's lower mantle should be a marked attenuation of seismic waves.

Keywords: $CaTiO_3$-$SrTiO_3$ solid solution, phase transitions, superattenuation, Resonant Ultrasound Spectroscopy

1. Introduction

The $CaTiO_3$-$SrTiO_3$ (CST) perovskite solid solution has attracted interest over a prolonged period for the diversity of structural variants and phase transitions which occur within it. A recently proposed phase diagram is reproduced in Figure 1, after Carpenter et al. (2006a). For Ca-rich compositions, the sequence of transitions with falling temperature is $Pm\bar{3}m$ ↔ *I*4/*mcm* ↔ *Pnma*. For compositions between ~$Ca_{0.4}Sr_{0.6}TiO_3$ and ~$Ca_{0.15}Sr_{0.85}TiO_3$, the sequence changes to $Pm\bar{3}m$ ↔ *I*4/*mcm* ↔ *Pbcm*. Stability fields for *Imma* or *Pnma* structures have also been proposed for Sr-rich compositions (Ranjan and Pandey, 1999, 2001a; Ranjan et al., 2000; Mishra et al., 2001; Ouillon et al., 2002; Ranson et al., 2005; Mishra et al., 2005, 2006a), and there has been a further suggestion of monoclinic symmetry (Woodward et al., 2006). From an earth sciences perspective, the CST solid solution has

ACCEPTED MANUSCRIPT

attracted interest as a potential analogue system for the structure, properties and behaviour of $(Mg,Fe)SiO_3$ and $CaSiO_3$ perovskites at high pressures and temperatures (Qin et al., 2000, 2002; Carpenter et al., 2001, 2007; Harrison et al., 2003; Carpenter, 2007a,b). In this context, the most significant issues relate to how the elastic properties vary with pressure, temperature and structure type and, in particular, to whether there are any anomalies in elastic constants or mechanical quality factor, Q, which might lead to a better understanding of the seismic properties of the lower mantle.

In this paper, the sequences of structures as a function of temperature and composition given by Carpenter et al. (2006a) are adopted, and $Pm\bar{3}m \leftrightarrow I4/mcm$, $I4/mcm \leftrightarrow Pnma$, $I4/mcm \leftrightarrow Pbcm$ transitions are referred to as T1, T2 and T3, respectively. Harrison et al. (2003) discovered strong anelastic effects associated with mobile twin walls in polycrystalline samples of CST at low frequencies of applied stress ($\sim 10^0$-10^2 Hz) by Dynamical Mechanical Analysis (DMA). They showed that there is an interval of temperature below T1 within which Young's modulus reduces to ~10% of the value for the cubic phase and that this superelastic softening is accompanied by significant dissipation, $\tan\delta$. Below ~400-450 K in the stability field of the $I4/mcm$ structure, the Young's modulus recovers and dissipation diminishes, which Harrison et al. (2003) interpreted as being due to pinning of mobile twin walls by oxygen vacancies. At T2 the elastic properties revert abruptly to those of a more normal elastic perovskite sample with minimal contributions from anelastic effects. This is in spite of the fact that crystals with $Pnma$ symmetry should still contain transformation twins. Polycrystalline samples prepared by hot pressing have also been examined at room temperature and in-situ at high pressures by the pulse-echo ultrasonic method at frequencies of ~10-70 MHz (Carpenter et al., 2007). The same pattern of stiff cubic and orthorhombic samples plus soft tetragonal samples was observed at room temperature. However, the pattern of evolution of the shear modulus through T1 did not match that predicted using a Landau

ACCEPTED MANUSCRIPT

free energy expansion which had been calibrated using the large amount of experimental data available for $SrTiO_3$ (Carpenter, 2007a,b). Furthermore, it is known that twin walls are mobile down to at least ~40 K in $SrTiO_3$ at low frequencies of applied stress (Schranz et al., 1999; Kityk et al., 2000a, b; Lemanov et al., 2002), and that the elastic properties of twinned samples measured at MHz frequencies are different from those obtained from within a single tetragonal twin domain by Brillouin scattering (as summarised in Carpenter, 2007a). Open questions evidently remain with regard to the influence of phase transitions and transformation twinning through T1 and below the temperature interval of domain wall pinning.

In the present study the elastic properties of CST perovskites have been investigated by Resonant Ultrasound Spectroscopy (RUS), a well established technique for measuring elastic constants of crystals at frequencies of ~10^5-10^6 Hz and over wide temperature intervals (e.g. Migliori and Sarrao, 1997). RUS was chosen because it allows values of bulk modulus (K), shear modulus (G) and mechanical quality factor (Q) to be determined simultaneously for polycrystalline samples. An important additional difference from other mechanical methods is in the strains involved. Anecodotal evidence among some practitioners of RUS is that the magnitudes of induced strains are ~10^{-7}-10^{-8}, though the actual values depends on the mass of the sample, the mass of the backloads, sample size and elastic stiffness, and the response of the small cross-section where the corner of the sample meets the driving piezoelectric crystal. That this estimate is not too far from reality appears to be confirmed by laser-Doppler interferometry data of Ogi et al. (2004), who found that the maximum surface displacement of a parallelepiped of α-TeO_2 with dimensions ~7x7x9 mm was ~1nm. The shear strain along a 7mm long edge with a maximum displacement of 1 nm at its centre corresonds to a maximum shear strain of ~3 x 10^{-7}. Strains of this order are directly comparable with the strains which pertain in seismic waves (10^{-6}-10^{-8}, Karato and Spetzler, 1990) and are substantially smaller

ACCEPTED MANUSCRIPT

than those induced in DMA or torsion pendulum experiments (~10^{-3}-10^{-5}, Harrison and Redfern, 2002; Lemanov et al., 2002). RUS data should therefore provide an additional perspective on dispersion with respect to both frequency and stress for anelastic effects due to twin wall motions. Figure 1 shows that the compositions and temperature intervals selected for investigation include the principal structure types of CST perovskites (i.e. $Pm\bar{3}m$, $I4/mcm$, $Pnma$, $Pbcm$), and cross each of the T1, T2 and T3 transitions between them. As well as presenting elasticity data for the CST system, the implications of analogue behaviour for silicate perovskites are considered. Strong support is provided for the original suggestion of Harrison and Redfern (2002) and Harrison et al. (2003) that the seismic signature for tetragonal $CaSiO_3$ in the mantle should be significant attenuation of shear waves.

2. Preparation and characterisation of samples

Samples of polycrystalline CST were produced from synthetic powders prepared originally for the study of Carpenter et al. (2007). The compositions selected for study were $CaTiO_3$ (CST0), $Ca_{0.7}Sr_{0.3}TiO_3$ (CST30), $Ca_{0.5}Sr_{0.5}TiO_3$ (CST50), $Ca_{0.3}Sr_{0.7}TiO_3$ (CST70), $Ca_{0.2}Sr_{0.8}TiO_3$ (CST80) and $Ca_{0.05}Sr_{0.95}TiO_3$ (CST95). Either ~3 or ~4 grams of each powder was pressed under vacuum (generated using a rotary pump) for ~5 minutes at 2-4 tonnes pressure in a steel die. The pressed pellets were fired for ~48 hours in air at ~1600 °C, followed by cooling to room temperature at 3 °C per minute. They emerged as brown discs with thicknesses of 5-9 mm and diameters of ~12 mm. Parallelepipeds with edge lengths in the range ~2-5 mm were cut from these using a fine (~300 μm) annular diamond saw, with paraffin as lubricant.

Dimensions of the parallelepipeds were measured with a hand held micrometer to a precision of ± 0.001 mm and weighed on a standard balance to a precision of ± 0.0001 gm. Densities obtained using these measured parameters were compared with theoretical densities

ACCEPTED MANUSCRIPT

calculated using the room temperature lattice parameter data of Ball et al. (1998), in order to obtain an estimate of porosity. Data for dimensions, mass, density and porosity of all the parallelepipeds are given in Table 1.

A portion of each fired pellet was ground up for investigation by powder X-ray diffraction using a Bruker D8 Advance diffractometer ($CuK\alpha_1$ radiation). Sharp, strong peaks of CST perovskite dominated the diffraction patterns from all six samples. A single, weak peak corresponding to the strongest peak of rutile was also present in the diffraction pattern from CST0. As a further characterisation measure, parts of the pressed pellets were prepared as thin sections for examination in a petrographic microscope. The CST0 sample contained birefringent grains on a scale of ~250 μm and these contained lamellar twins on a scale of ~10 μm. Many of the grain boundaries were decorated with a thin film of a highly birefringent material, which was assumed to be rutile on the basis of the powder diffraction evidence. Grain sizes of the CST30, CST50, CST70 and CST80 samples appeared to be substantially smaller, at ~25 μm. However, the birefringence of these was very low and it was not possible clearly to identify individual crystals. Some grain boundaries were decorated by a thin birefringent film, which, by analogy with the observations on CST0, perhaps indicate the presence of trace amounts of rutile. The CST95 sample was not examined in thin section but should be similar in character to the other samples with intermediate compositions across the solid solution.

3. RUS data collection and analysis

Room temperature RUS spectra were recorded in Cambridge using M^3odulus II (Dynamic Resonance System) driving electronics and a sample holder containing 2MHz compressional mode PZT-5 piezoceramics. Spectra containing 20,000 data points in the frequency range 300-1500 kHz were transferred to the software package IGOR Pro

ACCEPTED MANUSCRIPT

(WaveMetrics) for analysis. Frequencies of resonance peaks were obtained by inspection and the widths of selected peaks at half maximum were obtained by fitting with an asymmetric Lorentzian function. The frequencies of at least 20 (generally 30-40) peaks were used as input for the DRS software to calculate values of bulk (K) and shear (G) moduli. The methodology used in this software is described in Migliori and Sarrao (1997). Estimated uncertainties for the calculated values of G were generally less than 0.06% and always less than 0.3%. Owing to the fact that fewer resonance peaks contain information about K, estimates for the uncertainties in calculated values of the bulk modulus were higher, at 0.25-1.14%. Values of Q were determined as $\omega/\Delta\omega$, where ω is the frequency and $\Delta\omega$ the width at half maximum of a single peak, from fitting of the asymmetric Lorentzian profile. Where possible, the second peak in each spectrum was used to determine Q, and this depended on approximately 85% of G and 15% of K. Table 1 contains data for elastic properties at room temperature.

RUS spectra were collected *in situ* at high temperatures for CST0 (299-1677 K) and CST50 (299-1123 K) in Frankfurt using the instrument described by Schreuer and Haussühl (2005) and Schreuer et al. (2006). Parallelepipeds were held across opposite corners between horizontal alumina rods inside a sliding furnace which permitted temperature control to ~ ±0.1 K. Spectra were recorded at 100 K intervals away from transition points and at 5 K intervals within 20 K of T1 and T2. As an illustration of the primary high temperature data, spectra for CST50 are shown in Figure 2a. Peak positions were again used to calculate values of G and K, in this case following the methodology described by Schreuer (2002), Schreuer and Thybaut (2005) and Schreuer et al. (2006). Linewidths were determined using the asymmetric Lorentzian peak-fitting procedure of Schreuer et al. (2003) and Schreuer and Thybaut (2005), in order to obtain values of Q. The effects of thermal expansion are expected to be small in comparison with changes in the intrinsic elastic constants with temperature and changes due to phase transitions. Thermal expansion parameters were nevertheless

ACCEPTED MANUSCRIPT

determined for CST0 and CST50 samples in Frankfurt by dilatometry. Using the correct dimensions and density at high temperatures yielded values of *G* and *K* which were still within the original experimental uncertainty limits, however, so room temperature values of parallelepiped dimensions and density were used in calculations of all the elastic constant data presented here. The first CST0 parallelepiped used gave an unexpected reduction in *Q* with falling temperature in the stability field of the *Pnma* structure. A second parallalepiped of this sample was therefore examined on a similar high temperature RUS instrument in Cambridge, with the same driving electronics as used for the room temperature measurements.

Low temperature spectra were collected in Cambridge for samples CST70 (129→291 K) and CST95 (203→293 K) using an RUS sample holder placed inside a helium cryostat, as described in McKnight et al. (2007). The sample chamber was first evacuated and then filled with ~200 mbar of He to allow heat exchange between sample and cryostat. Temperature was controlled with a silicon diode temperature sensor and Lakeshore 340 controller to a precision and stability of ±0.1 K. Spectra containing 20,000 data points were collected in the frequency range 300-1400 kHz and are illustrated for CST70 in Figure 2b. The frequencies of at least 15 resonance peaks were used to calculate values of *K* and *G*, as described above for the room temperature data. Values of *Q* were obtained from the second peak in each spectrum or from an adjacent intense peak.

In order to generate values of *K* and *G* for comparison with pulse-echo ultrasonic data obtained from hot-pressed samples with ~0% porosity (Carpenter et al., 2007), it was necessary to make a correction to describe the influence of the 5-9% porosity of the RUS samples. To this end, values of the observed bulk and shear moduli, together with the estimated porosities for each parallelepiped were inserted into expressions given by Ledbetter et al. (1994):

Accepted Manuscript

ACCEPTED MANUSCRIPT

$$K = K_o \frac{4(1-c)G_o}{4G_o + 3cK_o}$$

$$G = G_o \frac{(1-c)(9K_o + 8G_o)}{(9+6c)K_o + (8+12c)G_o}.$$

K_o and G_o are the values for fully dense polycrystalline samples and c is the fractional porosity of the actual sample from which K and G were measured. Bulk and shear moduli corrected for porosity in this way are listed alongside the raw data in Table 1 for room temperature. Results shown in Figures 3-7 are either raw or corrected data, as specified below and in the figure captions.

Deviations from the Cauchy relation (Poisson's ratio = 1/4) have been calculated using the room temperature data corrected for porosity as $g = C_{12}–C_{44} = K_o–(5/3)G_o$, and are also listed in Table 1.

4. Experimental results

Room temperature values of K and G, corrected for porosity, are compared in Figure 3a with data from Carpenter et al. (2007) obtained by pulse-echo ultrasonics on dense samples. The two sets of data show similar patterns of systematic variation with composition for the shear modulus and a degree of scatter for the bulk modulus. Data for Q from the present study are shown in Figure 3b. CST100 (pure $SrTiO_3$) and CST95 are expected to be cubic at room temperature and both have $G \approx 116$ GPa, in agreement with other data from the literature (Table 2). CST70 and CST80 are expected to have the *I*4/*mcm* structure at room temperature (Fig. 1); both have lower values of G (~85 GPa) and Q (<400) than CST100 and CST95. CST30 and CST50 lie within the stability field of the *Pnma* structure and have values of G which are intermediate between those of the cubic and tetragonal samples. They also have high values of Q comparable with cubic samples. CST0 (pure $CaTiO_3$) has $G \approx 105$ GPa, in agreement with other data from the literature (Table 2), but a value of Q which is

ACCEPTED MANUSCRIPT

significantly lower than those of the other *Pnma* samples (CST30, CST50). Deviations from Cauchy relations are also systematic at room temperature in that cubic samples have *g* large and negative, tetragonal samples have *g* large and positive while orthorhombic samples have relatively small values of *g* (Table 1).

Results for CST0 (*K*, *G* uncorrected for porosity, and *Q*) at high temperatures are shown in Figure 4. Both *K* and *G* decrease as the *I*4/*mcm* ↔ *Pnma* transition (T2) is approached. All resonances disappeared from spectra collected within the stability field of the *I*4/*mcm* structure and remained absent up to the highest temperature achieved, 1621 K. Peaks reappeared on cooling but their pattern was different, implying that some irreversible changes had occurred. The sample was examined after cooling to room temperature and had clearly undergone a degree of surface recrystallisation. This first sample also showed an unusual pattern of variation for *Q* during heating, with a clear maximum in the vicinity of ~1000 K. The low values of *Q* between room temperature and ~600 K, followed by a steep rise between ~600 and ~800 K, were confirmed for the second parallelepiped on the Cambridge high temperature instrument (Fig.4b).

High temperature data for CST50, uncorrected for porosity, are shown in Figure 5. The most striking feature of the behaviour of this sample was the disappearance of all resonance peaks from spectra collected between T1 and T2, i.e. in the stability field of the *I*4/*mcm* structure. Values of *K* and *G* are similar above T1 and below T2, indicating that the elastic properties of the cubic and orthorhombic forms are similar. There was some decrease in *Q* as T2 was approached from below (Fig. 5b), as observed also for CST0 (Fig. 4b).

Low temperature data for CST70 (uncorrected for porosity) are shown in Figure 6. The *I*4/*mcm* ↔ *Pbcm* transition (T3) is marked by a slight change in the trend for *G*, perhaps with a small discontinuity (Fig. 6a). The bulk modulus appears to be unaffected. Much more

Accepted Manuscript

ACCEPTED MANUSCRIPT

significant changes occur in Q, however, with low values in the $I4/mcm$ stability field being replaced by high values in the *Pbcm* stability field (Fig. 6b).

Figure 7a contains data for K and G from the present study for CST95 at low temperatures (corrected for porosity) and data for $SrTiO_3$ from Figure 9 of Carpenter (2007b). The latter are Voigt/Reuss/Hill averages of single crystal data obtained using pulse-echo ultrasonics by Rehwald (1970) and Lei (1991). The pattern of variation of G for CST95 and CST100 is essentially the same, with some softening just above the $Pm\bar{3}m \leftrightarrow I4/mcm$ transition (T1) and an abrupt change at T1 itself. The magnitude of the discontinuity is the same for both samples and gives values for tetragonal samples which lie below those expected on the basis of a Landau model of the transition (broken line in Fig. 7a). As before for all other samples, there is no convincing evidence of any influence of the phase transition on the temperature evolution of the bulk modulus of CST95. Q shows an abrupt reduction in the stability field of the $I4/mcm$ structure (Fig. 7b).

5. Discussion

A prime motivation for undertaking this study was to investigate elastic and anelastic anomalies associated with phase transitions in CST perovskites which might provide additional insights into the possible behaviour of $(Mg,Fe)SiO_3$ and $CaSiO_3$ perovskites at depth in the earth. While the analogies will only be qualitative, a distinctive pattern of elastic behaviour is clear from the new RUS data presented here when combined with the low frequency measurements of Harrison et al. (2003) and the high frequency measurements of Carpenter et al. (2007). Firstly, any anomalies in the bulk modulus are small. This is because the coupling of volume strains with the order parameter for octahedral tilting transitions in perovskites is generally weak. Carpenter (2007a) used the strain analysis approach of Carpenter et al. (2001) to show that the bulk modulus might reduce by a few %, at most, for

ACCEPTED MANUSCRIPT

$SrTiO_3$ on transforming from $Pm\bar{3}m$ to $I4/mcm$ symmetry. A sharp discontinuity is expected at the transition point, with some softening as it is approached from the stability field of the cubic phase, but the data for this transition as a function of composition are too scattered to resolve such changes (Fig. 3a). Data for CST95 as a function of temperature (Fig. 7a) and as a function of pressure (Carpenter et al., 2007) through T1 also do not reveal any obvious discontinuity. One consideration in dealing with twinned crystals, however, is that the twin walls could act as stiff braces in a softer matrix (Carpenter, 2007b), so acting to reduce the total amount of softening expected for crystals without twins. There is also no reason to suppose that an anomaly in the bulk modulus at the $I4/mcm \leftrightarrow Pnma$ transition would be any larger than at the $Pm\bar{3}m \leftrightarrow I4/mcm$ transition. However, significant changes have been found in the evolution of the shear modulus with temperature and composition which show that the tetragonal phase of CST has elastic properties which are quite different from the those of the cubic and orthorhombic phases.

The distinctive characteristics of CST perovskites with $I4/mcm$ symmetry are, (a) that they are elastically softer with respect to pure shear than either of the $Pm\bar{3}m$ or $Pnma$ forms, (b) that they display significantly larger values of the deviations from Cauchy relations in comparison with cubic and orthorhombic forms, and (c) that they cause substantial anelastic dissipation both above and below the temperature interval of domain wall freezing found by Harrison et al. (2003). Deviations from Cauchy relations are usually understood in terms of the dominance of different types of bonding (Haussühl, 1967; Schreuer and Haussühl, 2005). Negative values indicate a dominance of directional bonding (covalent interactions, for example), whereas strongly positive values occur in crystals with non-directional bonding (dominance of Coulombic interactions). On this basis non-directional bonding effects are more important in the tetragonal structure than in either of the cubic or orthorhombic

Accepted Manuscript

ACCEPTED MANUSCRIPT

structures, but the significance of this observation for the rest of the elastic behaviour is not considered further here.

The most notable feature of the *I*4/*mcm* stability field at high temperatures is that resonance peaks are totally attenuated (CST50, Fig. 2a). Similar dissipative effects have been observed in rhombohedral $LaAlO_3$ and have been referred to as "superattenuation" by Carpenter et al. (2006b) because they occur in the same temperature interval as "superelastic" softening associated with twin wall motions (Harrison and Redfern, 2002). The temperature interval of superelastic softening in CST perovskites extends from T1 down to ~400-450 K for measurements made at frequencies of 1-320 Hz (Harrison et al., 2003). The polycrystalline samples of Harrison et al. (2003) also yielded values of $\tan\delta$ (= Q^{-1}) up to ~0.06 in this interval. In the present study, the resolution of RUS spectra is such that peaks with $Q \leq$ ~50 would probably not be observed, corresponding to $Q^{-1} \geq$ ~0.02. Anelastic behaviour at ~10^0-10^2 and ~10^6 Hz is thus rather similar, implying that the principal underlying mechanism, i.e. twin wall relaxations, could be the same. The working hypothesis behind the interpretation presented here, therefore, is that the timescale for twin wall relaxations can be shorter than ~10^{-6} s. Below the expected twin wall freezing temperature interval, *I*4/*mcm* phases of CST70 and CST95 gave observable peaks in RUS spectra but *Q* remained a factor of 3-10 below the values typically observed for cubic and orthorhombic samples (Fig. 3b, 6b, 7b). In this range the observed values of *G* from RUS, pulse-echo ultrasonics and perhaps also from DMA (Carpenter, 2007b) are significantly below those expected on the basis of a fully parameterised Landau description of the $Pm\bar{3}m \leftrightarrow I4/mcm$ transition (Fig. 3a). Thus it appears that the pinning process may only be partial, and that some degree of anelastic, twin wall mediated softening remains possible.

In general, the magnitude of anelastic softening due to twin wall movements under applied stresses depends largely on the restoring force they experience when they become

ACCEPTED MANUSCRIPT

displaced from their stress-free configurations, while the magnitude of dissipation depends largely on viscous drag as they move (Combs and Yip, 1983; Huang et al., 1992; Harrison and Redfern, 2002; Harrison et al., 2003, 2004). Between T1 and the freezing interval, tetragonal crystals are most likely to be in the domain wall sliding regime of Natterman et al. (2001) when subject to the relatively high stresses of three point bending in Dynamical Mechanical Analysis. In an RUS experiment, the induced strains are likely to be ~100-1000 times smaller but the twin walls appear still to be mobile. If there is a critical stress required to initiate domain wall sliding, it may be below the stresses involved even in seismic waves. From both frequency and stress perspectives, therefore, elastic softening and attenuation by this mechanism should occur when a seismic wave passes through a polycrystalline, twinned, tetragonal sample. A pinned twin wall can still be free to move between pinning points (Nattermann et al., 1990, 2001), and for low temperature/low stresses there is also the possibility of local thermally activated motions on a similarly small length scale, giving rise to domain wall creep (Nattermann et al., 2001). Whether this relates to the mechanism that pertains in CST below the freezing interval remains to be determined but it would account for the anelastic softening and dissipation which is additional to the normal effects of strain/order parameter coupling described by Landau theory.

Harrison et al. (2003) found that *Pnma* CST samples show no obvious signs of anelastic behaviour and concluded that the twin walls do not move under an externally applied stress once the symmetry is reduced below tetragonal. They commented on the fact that *Pnma* samples at intermediate compositions in the CST solid solution have pseudocubic lattice geometry (Carpenter et al. 2001), which means that there will be no resolved shear stress on the twin walls (see, also, discussion in Carpenter et al., 2007). It is not universally the case that twin walls are immobile in *Pnma* perovskites, however, since Daraktchiev et al. (2006) reported anelastic phenomena in the *Pnma* form of $Sr_{0.8}Ca_{0.2}SnO_3$. The unusual drop

ACCEPTED MANUSCRIPT

in Q below ~800 K in $CaTiO_3$ (Fig. 4b) and with $CaTiO_3$ enrichment across the CST solid solution at room temperature (Fig. 3b) might therefore be indicative of the onset of some degree of twin wall motion. In this context, perhaps there is some significance in the variation of high temperature lattice parameter data given by Kennedy et al. (1999) for $CaTiO_3$, in that the tetragonal strain which is close to zero between T2 and ~800 K becomes larger in magnitude below ~800 K (see Fig. 5 of Carpenter et al., 2001). Once there is a finite tetragonal strain, there will be a resolved shear stress on the twin walls for most orientations of an externally applied stress. The shear strain e_4 remains significant over the full temperature range of the *Pnma* stability field, however. Webb et al. (1999) did not find similar evidence of dissipation in $CaTiO_3$ at 50 MHz, and the behaviour of orthorhombic perovskites remains a topic of on-going research.

The *Pbcm* structure of CST can be described as occurring by coupling of octahedral tilts associated with irreducible representations R^{4+} and T_4 of space group $Pm\bar{3}m$ (Carpenter et al., 2006a). It differs also from the *Pnma* structure by having antiferroelectric atomic displacements (Ranjan and Pandey, 2001b; Mishra et al., 2002, 2006b; and see discussion in Carpenter et al., 2006a). Continuing to interpret the observed behaviour in terms of twin wall motions leads to the conclusion that the abrupt increase in Q at the $I4/mcm \rightarrow Pbcm$ transition (Fig. 6) is due to the twin walls becoming effectively immobile. The tetragonal strain e_t does not go to zero in the *Pbcm* phase of CST70 (see Fig. 6 of Carpenter et al., 2006a), so that a change in the viscous drag associated with the antiferroelectric character of the structure could be implicated.

If it is now assumed, following the work of Harrison and Redfern (2002) and Harrison et al. (2003), that the properties and behaviour of twin walls in tetragonal CST and rhombohedral $LaAlO_3$ perovskites are not fundamentally different from those of any other perovskites which undergo octahedral tilting transitions, some generalisations can be made

ACCEPTED MANUSCRIPT

about the likely seismic properties of silicate perovskites. Experimental data for $CaSiO_3$ place the $Pm\bar{3}m \leftrightarrow I4/mcm$ transition in the vicinity of the lower mantle geotherm (Ono et al., 2004a; Kurashina et al., 2004; Caracas et al., 2005; Jung and Oganov, 2005; Li et al. 2006a, b; Adams and Oganov, 2006; and references therein). If the geotherm passes only through the stability field of the cubic phase, the elastic properties should be normal, i.e. with high Q. If it passes through the transition line in PT space there should be a marked discontinuity in the shear modulus or, at least, a reduction in G of perhaps tens of % over a narrow PT range. Twin walls must almost inevitably be present in the tetragonal phase, from which it follows that there will also be significant attenuation. In the domain wall sliding regime, $Q << 50$ is expected for both low frequencies and low stresses. Below the freezing interval, values of $Q <$ 400, or at least lower by a factor of 3 or more than for untwinned crystals are likely, even without taking into account the additional effects of grain boundaries and dislocations. The characteristic seismic signature of tetragonal $CaSiO_3$ in the lower mantle should therefore be significant attenuation, whether the PT conditions are below or above the freezing interval. $(Mg,Fe)SiO_3$ is widely believed to be in the *Pnma* stability field at lower mantle conditions (Wentzcovitch et al., 1993; Stixrude and Cohen, 1993; Fiquet et al., 1998; Ono et al. 2004b; and references therein). Depending on the tetragonal strain, twinning in this phase could potentially also cause significant attenuation. Critical parameters required to assess these predictions more quantitatively include the spontaneous strains of $(Mg,Fe)SiO_3$ and $CaSiO_3$ at simultaneous high pressures and temperatures, the concentration of oxygen vacancies (a function of oxygen fugacity) and the activation volume for oxygen vacancy migration, which will determine the pressure dependence of the twin wall freezing temperature. The closer the tetragonal phases are to the $Pm\bar{3}m \leftrightarrow I4/mcm$ transition, the more likely they are to be in the domain wall sliding regime even at the low frequencies and low stresses of seismic waves.

Accepted Manuscript

ACCEPTED MANUSCRIPT

Acknowledgements

The Cambridge RUS facility was established with a grant from the Natural Environment Research Council (grant no. NE/B505738/1), which is gratefully acknowledged.

References

Adams, D.J., Oganov, A.R., 2006. Ab initio molecular dynamics study of $CaSiO_3$ perovskite at P-T conditions of Earth's lower mantle. Phys. Rev. B 73, 184106.

Ali, R., Yashima, M., 2005. Space group and crystal structure of the perovskite $CaTiO_3$ from 296 to 1720 K. J. Solid State Chem. 178, 2867–2872.

Ball, C.J., Begg, B.D., Cookson, D.J., Thorogood, G.J., Vance, E. R., 1998. Structures in the system $CaTiO_3/SrTiO_3$. J. Solid State Chem. 139, 238–247.

Bell, R.O., Rupprecht, G., 1963. Elastic constants of strontium titanate. Phys. Rev. 129, 90–94.

Caracas, R., Wentzcovitch, R., Price, G.D., Brodholt, J., 2005. $CaSiO_3$ perovskite at lower mantle pressures. Geophys. Res. Lett. 32, L06306.

Carpenter, M.A., Becerro, A.I., Seifert, F., 2001. Strain analysis of phase transitions in $(Ca,Sr)TiO_3$ perovskites. Am. Mineral. 86, 348–363.

Carpenter, M.A., Howard, C.J., Knight, K.S., Zhang, Z., 2006a. Structural relationships and a phase diagram for $(Ca,Sr)TiO_3$ perovskites. J. Phys. Condens. Matter 18, 10725–10749.

Carpenter, M.A., Darling, T.W., Bass, J.D., Lakshtanov, D.L., Sinogeikin, S.V., Jacobsen, S.D., 2006b. Superattenuation of acoustic resonances and non-linear elasticity associated with the cubic-rhombohedral phase transition in $LaAlO_3$ perovskite. Eos Trans. AGU 87(52), Fall Meet. Suppl. Abstract MR34A-01.

Accepted Manuscript

ACCEPTED MANUSCRIPT

Carpenter, M.A., Li, B., Liebermann, R.C., 2007. Elastic anomalies accompanying phase transitions in (Ca,Sr)TiO_3 perovskites: Part III. Experimental investigation of polycrystalline samples. Am. Mineral. 92, 344–355.

Carpenter, M.A., 2007a. Elastic anomalies accompanying phase transitions in (Ca,Sr)TiO_3 perovskites: Part I. Landau theory and a calibration for $SrTiO_3$. Am. Mineral. 92, 309–327.

Carpenter, M.A., 2007b. Elastic anomalies accompanying phase transitions in (Ca,Sr)TiO_3 perovskites: Part II. Calibration for the effects of composition and pressure. Am. Mineral. 92, 328–343.

Combs, J.A., Yip, S., 1983. Single-kink dynamics in a one-dimensional atomic chain: a nonlinear atomistic theory and numerical simulation. Phys. Rev. B 28, 6873–6885.

Daraktchiev, M., Harrison, R.J., Mountstevens, E.H., Redfern, S.A.T., 2006. Effect of transformation twins on the anelastic behavior of polycrystalline $Ca_{1-x}Sr_xTiO_3$ and $Sr_xBa_{1-x}SnO_3$ perovskite in relation to the seismic properties of Earth's mantle perovskite. Mat. Sci. Eng. A 442, 199–203.

Fiquet, G., Andrault, D., Dewaele, A., Charpin, T., Kunz, M., and Haüsermann, D., 1998. P-V-T equation of state of $MgSiO_3$ perovskite. Phys. Earth Planet. Int. 105, 21–31.

Fischer, G.J., Wang, Z., Karato, S.-I., 1993. Elasticity of $CaTiO_3$, $SrTiO_3$ and $BaTiO_3$ perovskites up to 3.0 GPa: the effect of crystallographic structure. Phys. Chem. Min. 20, 97–103.

Harrison, R.J., Redfern, S.A.T., 2002. The influence of transformation twins on the seismic-frequency elastic and anelastic properties of perovskite: dynamical mechanical analysis of single crystal $LaAlO_3$. Phys. Earth Planet. Int. 134, 253–272.

Accepted Manuscript

ACCEPTED MANUSCRIPT

Harrison, R.J., Redfern, S.A.T., Street, J., 2003. The effect of transformation twins on the seismic-frequency mechanical properties of polycrystalline $Ca_{1-x}Sr_xTiO_3$ perovskite Am. Mineral. 88, 574–582.

Harrison, R.J., Redfern, S.A.T., Bismayer, U., 2004. Seismic-frequency attenuation at first-order phase transitions: dynamical mechanical analysis of pure and Ca-doped lead orthophosphate. Miner. Mag. 68, 839–852.

Haussühl, S., 1967. Die Abweichungen von den Cauchy-Relationen. Phys. kondens. Mater. 6, 181–192.

Huang, Y.N., Wang, Y.N., Shen, H.M., 1992. Internal friction and dielectric loss related to domain walls. Phys. Rev. B 46, 3290–3295.

Jung, D.Y., Oganov, A.R., 2005. Ab initio study of the high-pressure behavior of $CaSiO_3$ perovskite. Phys. Chem. Min. 32, 146–153.

Karato, S., Spetzler, H.A., 1990. Defect microdynamics in minerals and solid state mechanisms of seismic wave attenuation and velocity dispersion in the mantle. Rev. Geophys. 28, 399–421.

Kennedy, B.J., Howard, C.J., Chakoumakos, B.C., 1999. Phase transitions in perovskite at elevated temperatures – a powder neutron diffraction study. J. Phys. Condens. Matter 11, 1479–1488.

Kityk, A.V., Schranz, W., Sondergeld, P., Havlik, D., Salje, E.K.H., Scott, J.F., 2000a. Low-frequency superelasticity and nonlinear elastic behavior of $SrTiO_3$ crystals. Phys. Rev. B 61, 946–956.

Kityk, A.V., Schranz, W., Sondergeld, P., Havlik, D., Salje, E.K.H., Scott, J.F., 2000b. Nonlinear elastic behaviour of $SrTiO_3$ crystals in the quantum paraelectric regime Europhys. Lett. 50, 41–47.

Accepted Manuscript

ACCEPTED MANUSCRIPT

Kurashina, T., Hirose, K., Ono, S., Sata, N., and Ohishi, Y., 2004. Phase transition in Al-bearing $CaSiO_3$ perovskite: implications for seismic discontinuities in the lower mantle. Phys. Earth Planet. Int. 145, 67–74.

Ledbetter, H., Lei, M., Hermann, A., Sheng, Z., 1994. Low-temperature elastic constants of $Y_1Ba_2Cu_3O_7$. Physica C 225, 397–403.

Lei, M., 1991. Oxides and oxide superconductors: elastic and related properties. Ph.D. dissertation, University of Colorado, Boulder.

Lemanov, V.V., Gridnev, S.A., and Ukhin, E.V. (2002) Low-frequency elastic properties, domain dynamics, and spontaneous twisting of $SrTiO_3$ near the ferroelastic phase transition. Phys. Solid State 44, 1156–1165.

Li, L., Weidner, D.J., Brodholt, J., Alfè, D., Price, G.D., Caracas, R., Wentzcovitch, R., 2006a. Elasticity of $CaSiO_3$ perovskite at high pressure and high temperature. Phys. Earth Planet. Int. 155, 249–259.

Li, L., Weidner, D.J., Brodholt, J., Alfè, D., Price, G.D., Caracas, R., Wentzcovitch, R., 2006b. Phase stability of $CaSiO_3$ perovskite at high pressure and temperature: insights from ab initio molecular dynamics. Phys. Earth Planet. Int. 155, 260–268.

Liebermann, R.C., Jones, L.E.A., Ringwood, A.E., 1977. Elasticity of aluminate, titanate, stannate and germanate compounds with the perovskite structure. Phys. Earth Planet. Int. 14, 165–178.

McKnight, R.E.A., Carpenter, M.A., Darling, T.W., Buckley, A., Taylor, P.A., 2007. Acoustic dissipation associated with phase transitions in lawsonite, $CaAl_2Si_2O_7(OH)_2.H_2O$. Am. Mineral. in press.

Migliori, A., Sarrao, J.L., 1997. Resonant ultrasound spectroscopy : applications to physics, materials measurements, and nondestructive evaluation. Wiley, New York, Chichester, 201 pp.

Accepted Manuscript

ACCEPTED MANUSCRIPT

Mishra, S.K., Ranjan, R., Pandey, D., Ouillon, R., Pinan-Lucarre, J.-P., Ranson, P., Pruzan, Ph., 2001. A Raman scattering study of the antiferrroelectric phase transition in $(Sr_{0.70}Ca_{0.30})TiO_3$. Phys. Rev. B 64, 092302.

Mishra, S.K., Ranjan, R., Pandey, D., Kennedy, B.J., 2002. Powder neutron diffraction study of the antiferroelectric phase transition in $Sr_{0.75}Ca_{0.25}TiO_3$. J. Appl. Phys. 91, 4447–4452.

Mishra, S.K., Ranjan, R., Pandey, D., Ranson, P., Ouillon, R., Pinan-Lucarre, J.-P., Pruzan, Ph., 2005. A combined X-ray diffraction and Raman scattering study of the phase transitions in $Sr_{1-x}Ca_xTiO_3$ (x = 0.04, 0.06, 0.12). J. Solid State Chem. 178, 2846–2857.

Mishra, S.K., Ranjan, R., Pandey, D., Stokes, H.T., 2006a. Resolving the controversies about the 'nearly cubic' and other phases of $Sr_{1-x}Ca_xTiO_3$ ($0 \le x \le 1$): I. Room temperature structures. J. Phys. Condens. Matter 18, 1885–1898.

Mishra, S.K., Ranjan, R., Pandey, D., Ranson, P., Ouillon, R., Pinan-Lucarre, J.-P., Pruzan, Ph., 2006b. Resolving the controversies about the 'nearly cubic' and other phases of $Sr_{1-x}Ca_xTiO_3$ ($0 \le x \le 1$): II. Comparison of phase transition behaviours for x = 0.40 and 0.43. J. Phys. Condens. Matter 18, 1899–1912.

Nattermann, T., Shapir, Y., Vilfan, Y., 1990. Interface pinning and dynamics in random systems. Phys. Rev. B 42, 8577–8586.

Nattermann, T., Pokrovsky, V., Vinokur, V.M., 2001. Hysteretic dynamics of domain walls at finite temperatures. Phys. Rev. Lett. 87, 197005.

Ogi, H., Fukunaga, M., Hirao, M., Ledbetter, H. 2004. Elastic constants, internal friction, and piezoelectric coefficient of α-TeO_2. Phys. Rev. B 69, 024104.

Ono, S., Ohishi, Y., Mibe, K., 2004a. Phase transition of Ca-perovskite and stability of Al-bearing Mg-perovskite in the lower mantle. Am. Mineral. 89, 1480–1485.

ACCEPTED MANUSCRIPT

Ono, S., Kikegawa, T., Iizuka, T., 2004b. The equation of state of orthorhombic perovskite in a peridotitic mantle composition to 80 GPa: implications for chemical composition of the lower mantle. Phys. Earth Planet. Int. 145, 9–17.

Ouillon, R., Pinan-Lucarre, J.-P., Ranson, P., Pruzan, Ph., Mishra, S.K., Ranjan, R., Pandey, D., 2002. A Raman scattering study of the phase transitions in $SrTiO_3$ and in the mixed system $(Sr_{1-x}Ca_x)TiO_3$ at ambient pressure from T = 300 K down to 8 K. J. Phys. Condens. Matter 14, 2079–2092.

Qin, S., Becerro, A.I., Seifert, F., Gottsmann, J., Jiang, J., 2000. Phase transitions in $Ca_{1-x}Sr_xTiO_3$ perovskites: effects of composition and temperature. J. Mater. Chem. 10, 1609–1615.

Qin, S., Wu, X., Seifert, F., Becerro, A.I., 2002. Micro-Raman study of perovskites in the $CaTiO_3$-$SrTiO_3$ system. J. Chem. Soc., Dalton Trans. 2002, 3751–3755.

Ranjan, R., Pandey, D., 1999. Novel structural features and phase transition behaviour of $(Sr_{1-x}Ca_x)TiO_3$: II. X-ray diffraction studies. J. Phys. Condens. Matter 11, 2247–2258.

Ranjan, R., Pandey, D., 2001a. Antiferroelectric phase transition in $(Sr_{1-x}Ca_x)TiO_3$: II. X-ray diffraction studies. J. Phys. Condens. Matter 13, 4251–4266.

Ranjan, R., Pandey, D., 2001b. Antiferroelectric phase transition in $(Sr_{1-x}Ca_x)TiO_3$ ($0.12 \leq x \leq 0.40$): I. Dielectric studies. J. Phys. Condens. Matter 13, 4239–4249.

Ranjan, R., Pandey, D., Lalla, N.P., 2000. Novel features of $Sr_{1-x}Ca_xTiO_3$ phase diagram: evidence for competing antiferroelectric and ferroelectric interactions. Phys. Rev. Lett. 84, 3726–3729.

Ranson, P., Ouillon, R., Pinan-Lucarre, J.-P., Pruzan, Ph., Mishra, S.K., Ranjan, R., Pandey, D., 2005. The various phases of the system $Sr_{1-x}Ca_xTiO_3$ - a Raman scattering study. J. Raman Spectrosc. 36, 898–911.

ACCEPTED MANUSCRIPT

Rehwald, W., 1970. Low temperature elastic moduli of strontium titanate. Solid State Com. 8, 1483–1485.

Schranz, W., Sondergeld, P., Kityk, A.V., Salje, E.K.H., 1999. Elastic properties of $SrTiO_3$ crystals at ultralow frequencies. Phase Transit. 69, 61–76.

Schreuer, J. 2002. Elastic and piezoelectric properties of $La_3Ga_5O_{14}$ and $La_3Ga_{5.5}Ta_{0.5}O_{14}$: an application of Resonant Ultrasound Spectroscopy. IEEE Trans. on Ultrasonics, Ferroelectrics and Frequency Control 49, 1474–1479.

Schreuer, J., Thybaut, C., Prestat, M., Stade, J., Haussühl, E., 2003. Towards an understanding of the anomalous electromechanical behaviour of langasite and related compounds at high temperatures. Proc. IEEE Ultrasonics Symp. 2003, 196–199.

Schreuer, J., Thybaut, C., 2005. Anelastic relaxation effects and elastic instabilities in CGG-type compounds. Proc. IEEE Ultrasonics Symp. 2005, 695–698.

Schreuer, J., Haussühl, S., 2005. Elastic and piezoelectric properties of minerals I. Principles and experimental approaches. EMU Notes in Mineralogy 7, 1–42.

Schreuer, J., Haussühl, S., 2005. Elastic and piezoelectric properties of minerals II. Structure-property relationships. EMU Notes in Mineralogy 7, 173–198.

Schreuer, J., Hildmann, B., Schneider, H., 2006. Elastic properties of mullite single crystals up to 1400 °C. J. Am. Ceram. Soc. 89, 1624–1631.

Sinelnikov, Y.D., Chen, G., Liebermann, R.C., 1998. Elasticity of $CaTiO_3$–$CaSiO_3$ perovskites. Phys. Chem. Min. 25, 515–521.

Stixrude, L., Cohen, R.E., 1993. Stability of orthorhombic $MgSiO_3$ perovskite in the earth's lower mantle. Nature 364, 613–615.

Webb, S., Jackson, I., Fitz Gerald, J., 1999. Viscoelasticity of the titanate perovskites $CaTiO_3$ and $SrTiO_3$ at high temperature. Phys. Earth Planet. Int. 115, 259–291.

Accepted Manuscript

ACCEPTED MANUSCRIPT

Wentzcovitch, R.M., Martins, J.L., Price, G.D., 1993. Ab initio molecular dynamics with variable cell shape: application to $MgSiO_3$. Phys. Rev. Lett. 70, 3947–3950.

Woodward, D.I., Wise, P.L., Lee, W.E., Reaney, I.M., 2006. Space group symmetry of $(Ca_xSr_{1-x})TiO_3$ determined using electron diffraction. J. Phys. Condens. Matter 18, 2401–2408.

Accepted Manuscript

ACCEPTED MANUSCRIPT

Table 1
Characterisation of parallelepipeds used in this study. Fractional porosity was estimated by comparing the observed densities with theoretical densities based on lattice parameter data of Ball et al. (1998). K and G are bulk and shear moduli measured at room temperature. K_o and G_o are bulk and shear moduli corrected for porosity. The Cauchy relation for an isotropic material is given in the last column as $g = K_o-(5/3)G_o$ (i.e. calculated using the values of K and G corrected for porosity).

Sample composn./no.	a (mm)	b (mm)	c (mm)	Mass (g)	Density (g.cm^{-3})	Fractional porosity	K (GPa)	G (GPa)	K_o (GPa)	G_o (GPa)	g (GPa)
CST0/1	3.773	4.271	4.771	0.2827	3.677	0.0885	139.4	88.1	169.1	104.8	-5.6
CST0/2	4.771	4.272	3.805	0.2852	3.678	0.0882	138.5	88.4	167.9	105.2	-7.4
CST0/3	3.805	4.272	4.771	0.2838	3.659	0.0930	138.6	88.8	169.8	106.7	-8.0
CST30/1	3.787	2.792	3.265	0.1388	4.031	0.0759	151.0	90.2	179.4	104.6	5.1
CST30/2	2.785	2.294	3.326	0.0847	4.005	0.0818	148.3	89.8	178.4	105.4	2.7
CST50/1	2.802	3.252	3.723	0.1445	4.259	0.0685	152.1	88.0	177.9	100.5	10.4
CST50/2	2.795	3.263	3.881	0.1510	4.266	0.0669	148.2	88.3	172.5	100.7	4.7
CST70/1	3.758	3.283	2.779	0.1571	4.582	0.0432	151.3	79.1	168.1	85.9	24.9
CST70/2	3.759	3.316	2.786	0.1584	4.562	0.0474	152.7	79.9	171.3	87.5	25.5
CST80/1	2.767	3.272	3.781	0.1555	4.543	0.0717	154.3	73.1	186.2	83.9	46.4
CST80/2	2.768	3.270	3.807	0.1568	4.550	0.0703	142.2	73.4	169.0	84.1	28.8
CST95/1	2.777	2.301	3.281	0.1000	4.770	0.0573	157.5	103.8	178.0	116.2	-15.7
CST100/1	2.410	1.763	4.787	0.0973	4.784	0.0651	142.0	101.3	162.3	115.3	-29.9
CST100/2	3.786	3.312	2.897	0.1765	4.859	0.0504	157.6	106.8	175.1	117.9	-21.4

Table 2
Comparison of room temperature shear and bulk moduli from the present study with data from the literature. Numbers in brackets indicate estimated uncertainties.

	K (GPa)	G (GPa)
$CaTiO_3$		
This study (corrected for porosity)	168.9[1] (0.8)	105.6[1] (0.8)
Webb et al. (1999)	172.1 (1.0)	102.0 (0.3)
Fischer et al. (1993)	176 (3)	105 (1)
Liebermann et al. (1977)	177 (3)	104 (1)
Sinelnikov et al. (1998)	175 (2)	107 (1)
Kung (1997), in Webb et al. (1999)	175	105
$SrTiO_3$		
This study (corrected for porosity)	169[2] (6)	116.6[2] (1.3)
Webb et al. (1999)	172 (1)	116.1 (0.3)
Fischer et al. (1993)	185 (5)	113 (2)
Bell and Rupprecht (1963)	174 (4)	117 (1)

[1]average of 3 measurements, [2]average of 2 measurements

Accepted Manuscript

ACCEPTED MANUSCRIPT

Figure captions

Fig.1. CST phase diagram from Carpenter et al. (2006a), showing the sample compositions at room temperature (stars) and high T ranges (solid lines) investigated in the present study.

Fig.2. Representative RUS spectra (a) collected at high temperatures for CST50 in Frankfurt and (b) collected at low temperatures for CST70 in Cambridge. The spectra are of amplitude vs. frequency but have been displaced along the y-axis so as to indicate their separation by temperature. Note that resonance peaks from the sample have disappeared from the three spectra collected within the stability field of the *I*4/*mcm* structure of CST50. Peaks in these spectra are from the rods which hold the sample across its corners.

Fig. 3. Variations of (a) bulk and shear moduli and (b) mechanical quality factor, as measured at room temperature. RUS data for K and G (filled circles) have been corrected for porosity. Open circles in (a) are pulse-echo ultrasonic data from Carpenter et al. (2007) and broken lines are a Landau description of the $Pm\bar{3}m \leftrightarrow I4/mcm$ transition from Carpenter (2007b). Crosses represent other data from the literature for $CaTiO_3$ and $SrTiO_3$. Composition limits for different structure types at room temperature (vertical dotted lines) are taken from Carpenter et al. (2006a).

Fig. 4. K, G (not corrected for porosity) and Q data for CST0. The transition temperatures shown are those of Ali and Yashima (2005); 1634 ± 13 K for T1 and 1498 ± 25 K for T2. It looks as though there is a systematic shift of transition temperatures in the present study, but this could simply be due to different temperature calibration between furnaces. Values of Q = 0 are shown in the *I*4/*mcm* stability field to signify that resonance peaks were absent from

ACCEPTED MANUSCRIPT

RUS spectra collected at these temperatures. Open symbols for Q represent data collected on a second parallelepiped on the Cambridge high temperature instrument.

Fig. 5. K, G (not corrected for porosity) and Q data for CST50. The transition temperatures shown are those from fits to the transition temperature data from the literature given in Carpenter et al. (2006a): ~925 K for T1 and ~580 K for T2. Values of $Q = 0$ are shown in the $I4/mcm$ stability field to signify that resonance peaks were absent from RUS spectra collected at these temperatures.

Fig. 6. K, G (not corrected for porosity) and Q data for CST70. The transition temperature for T3 ($I4/mcm \leftrightarrow Pbcm$), based on transition temperature data from the literature reviewed in Carpenter et al. (2006a), is ~230 K. This transition is first order in character and involves coexistence of the tetragonal and orthorhombic phases over a temperature interval of ~20-30 K. Note that two anomalous values of K have been left in the data set and signify that the surface representing fits to the data for bulk modulus is rather shallow and irregular.

Fig. 7. K, G (corrected for porosity) and Q for CST95 (filled circles), compared with data for $SrTiO_3$ taken from Carpenter (2007b). The transition temperature from fits to data for the $Pm\bar{3}m \leftrightarrow I4/mcm$ transition summarised in Carpenter et al. (2006a) is ~245 K at CST95. Solid lines are fits to data for cubic $SrTiO_3$ and broken lines are Landau solutions for tetragonal $SrTiO_3$. Crosses are Voigt/Reuss/Hill averages of single crystal data from ultrasonic measurements of Rehwald (1970) for $SrTiO_3$; open circles are data collected in a similar way by Lei (1991).

Accepted Manuscript

ACCEPTED MANUSCRIPT